2008

# Salt Marshes As a Source Of Chromophoric Dissolved Organic Matter (Cdom) To Southern California Coastal Waters

Catherine D. Clark
*Chapman University*

Liannea P. Litz
*Chapman University*

Stanley B. Grant
*University of California - Irvine*

Follow this and additional works at: http://digitalcommons.chapman.edu/sees_articles

Part of the Environmental Chemistry Commons, Oceanography Commons, and the Terrestrial and Aquatic Ecology Commons

# Salt Marshes As a Source Of Chromophoric Dissolved Organic Matter (Cdom) To Southern California Coastal Waters

# Salt marshes as a source of chromophoric dissolved organic matter (CDOM) to Southern California coastal waters

*Catherine D. Clark*[1] *and Liannea P. Litz*
Department of Chemistry, Chapman University, One University Drive, Orange, California, 92866

*Stanley B. Grant*
Henry Samueli School of Engineering, Department of Chemical Engineering and Materials Science, University of California, Irvine, California 92697

*Abstract*

To determine chromophoric dissolved organic matter (CDOM) sources in Southern California coastal waters, optical properties of a river outlet and adjacent tidally flushed salt marshes were monitored (dry season; June–July 2001). Average absorption coefficients doubled at ebb vs. flood tides ($4.8 \pm 1.5$ vs. $2.1 \pm 0.9$ m$^{-1}$; 300 nm), suggesting significant salt marsh CDOM inputs into coastal waters. Average spectral slopes were not statistically different for any sites or tides ($0.010 \pm 0.002$ nm$^{-1}$), consistent with salt marsh CDOM dominating coastal waters. Three-dimensional fluorescence excitation–emission matrices (EEMs) at ebb tide showed contributions from terrestrial, protein, and marine humic-like peaks, suggesting production and output of these materials from the marsh. A marine humic signal at the river outlet during an offshore upwelling event indicated an additional sporadic nonmarsh marine humic-like source. EEMs of six common salt marsh plant leachates showed protein, terrestrial, and marine humic-like peaks. To estimate CDOM photodegradation in the marsh, fluorescence intensity decays from photobleaching experiments were fit to first-order kinetics. Most humic peaks degraded with a half-life of $t_{1/2} = 10$–20 h, which overlaps the estimated residence time of water in the marshes ($\sim$12 h). Most protein peaks were resistant to photodegradation, suggesting that the low levels of protein vs. humic-like material measured in natural waters was due to rapid bioutilization of proteinaceous material. The rapid photodegradation of plant leachate humic material and the low spectral slopes for the field sites suggest that marsh sediments would be an important source of CDOM.

Dissolved organic matter (DOM) plays a critical role in a broad range of biogeochemical cycling processes in natural waters (Hessen and Tranvik 1998). The light-absorbing fraction of DOM, known as chromophoric dissolved organic matter (CDOM), affects ocean color, underwater light fields, and aquatic chemistry through a suite of sunlight-initiated photochemical processes (Miller 1998). CDOM is a highly complex macromolecular material containing humic substances (Hessen and Tranvik 1998). CDOM in coastal waters is dominated by inputs from rivers and wetlands of terrestrially derived materials from plant degradation, but lower levels of CDOM may also be produced from grazing phytoplankton and bacteria in marine and estuarine environments (McKnight and Aiken 1998; Rochelle-Newall and Fisher 2002).

Salt marshes are found in the middle and high latitudes in intertidal zones throughout the world (McLusky and Elliot 2004). North American estuarine salt marsh systems have long being recognized as being among the most productive ecosystems in the world (Mitsch and Gosselink 2000), with annual gross macrophyte aboveground primary production rates varying from 100 to 1000 g C m$^{-2}$ ($\sim$400 in Southern California). These high overall levels of production are attributed to the large supply of dissolved nutrients and vigorous production from plants in the intertidal zone (Mitsch and Gosselink 2000). Despite this high potential input of carbon from marshes, only a fraction of the gross primary production accumulates in the marsh ecosystem and becomes available for export to adjacent waters as DOM, particulate carbon, and biological production. Physical features such as tides, sediments, flow, and shoreline structure make the ultimate export of carbon to coastal waters variable from site to site (McLusky and Elliot 2004). However, in previous studies, most North American Atlantic and Gulf Coast marshes have been shown to be significant exporters of dissolved organic carbon to estuarine waters (McLusky and Elliot 2004), suggesting that tidal marshes act as an important local source of DOM in coastal waters. For example, Moran and Hodson (1994) estimated that up to 40% of DOM on the southeastern coastal shelf of the United States came from salt marshes. In a recent study of mangroves, a tropical intertidal system, Dittmar et al. (2006) showed that mangroves are the main source of

terrigenous DOC in the ocean off Brazil and estimated that mangroves account for >10% of terrestrial refractory DOC exported to the oceans.

However, little is known about the optical properties, composition, and processing of CDOM in marsh ecosystems. Because both the source and the photochemical and biological transformation processes alter the optical characteristics of CDOM, these optical properties have been used to differentiate between terrestrial and marine sources in saltwater and freshwater systems and between freshly produced and aged material from terrestrial sources (Miller and Moran 1997; Vodacek et al. 1997; Miller 1998). For example, spectral slopes, fluorescence : absorbance ratios, and three-dimensional (3D) excitation and emission fluorescence spectra have been used to evaluate the sources, distribution, and fate of CDOM (Coble 1996; Boyd and Osburn 2004; Obernosterer and Benner 2004).

Few studies of the optical properties of salt marsh–derived CDOM have been conducted in salt marshes, and most of these have focused on the Atlantic and Gulf Coast regions in the southeastern United States, where species nonnative to Southern California, like *Saltiplex*, dominate the ecosystem (Moran et al. 2000; Gallegos et al. 2005; Tzortziou et al. 2007). In tropical and semitropical zones, salt marshes are replaced by mangrove swamps, which have also been shown to be major exporters of optically distinctive CDOM (Moran et al. 1991; Clark et al. 2002; Maie et al. 2006). No studies to our knowledge have been published on the properties of CDOM from salt marshes in Southern California, which have distinct ecology to eastern continental marshes. In one study of engineered treatment wetlands on the West Coast of the U.S.A., Barber et al. (2001) concluded that these were a significant source of distinctive CDOM to the through-flowing effluent based on nuclear magnetic resonance and Fourier transform–infrared studies. In Southern California in the dry season (spring, summer, and fall), there are little to no river inputs into the coastal ocean (Grant et al. 2005), suggesting that natural and engineered salt marshes, wetlands, and tidally flushed river outlets must be the major source of CDOM to coastal waters in this region for much of the year.

In this study, we measured the optical properties of CDOM over several semidiurnal tidal cycles in the dry season in two Southern California salt marshes and the adjacent river outlet into the surf zone. Leachates of the most common salt marsh species from these sites were analyzed for optical properties and contributions to the marsh outflow CDOM signal. Residence times of CDOM in the marshes were modeled with a simple box model for mixing in a tidal salt marsh based on the tidal prism and the marsh volume. Photodegradation experiments were conducted to assess the stability of the salt marsh plant–derived CDOM optical properties under solar irradiation for the short residence times obtained from the mixing model. The objective was to assess whether salt marshes are a dominant source of optically distinctive CDOM to Southern California coastal waters and hence play a major role in controlling ocean color, light fields, and biogeochemical processes in these waters.
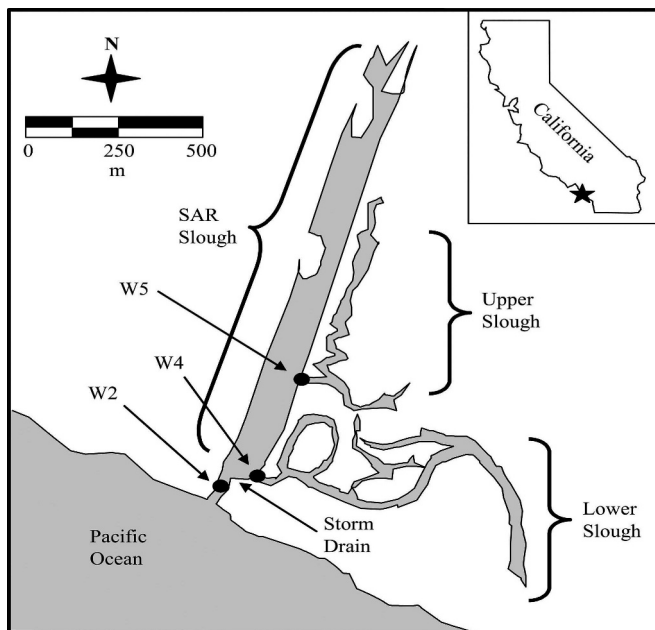


Fig. 1. Schematic diagram of the study site showing the location of the sampling stations (W2, W4, W5), the Lower Slough and Upper Slough, and the Santa Ana River outlet (SAR slough) in Orange County, California.

## Methods

*Sampling*—The Santa Ana River (SAR) outlet in Huntington Beach drains several moderately sized tidal saltwater marshes (~0.5 km²) and the SAR watershed (6900 km²), which encompasses Orange, San Bernadino, and Riverside counties in Southern California. In the summer months (June, July, and August, the dry season), there is little to no freshwater flow in the SAR upstream of the tidal prism. Like many Southern California "rivers," the SAR has been highly modified to minimize flooding by channelizing and lining much of the river with concrete. Water reclamation activities upstream of the tidal prism capture virtually all flow in the SAR in the dry season, so any freshwater added to the tidal prism during the dry season is from local sources of runoff (Grant et al. 2005). Flow-through the SAR outlet is tidally forced, with inflowing ocean water on a flood tide and outflowing water on an ebb tide (Grant et al. 2005). Figure 1 shows the three sites sampled for six tidal cycles between 26 June and 21 July 2001 (Fig. 1): station W5 (33°38.111′N, 117°57.298′W) located inside the tide gate at the upper slough outlet, station W4 (33°37.863′N, 117°57.390′W) located inside the tide gate at the lower slough outlet, and station W2 (33°37.835′N, 117°57.416′W) located underneath an overpass bridge, ~30 m upstream from where the SAR empties into the surf zone.

The sampling intervals relative to the daily and fortnightly tidal cycles have been previously published in a related study of fecal steroids carried out at this site over the same sampling period (Noblet et al. 2004). Samples of water entering the marshes (coastal-dominated waters) were sampled on a flood tide, and water draining the

marshes (marsh-dominated waters) were sampled on an ebb tide. A small oil field and a trailer park that houses a duck feeding station are on the shores of the Lower Slough (Fig. 1). Bulk integrated 20-liter samples were collected from each site using a stainless-steel bucket attached to an aluminum pole (1) at the peak of the flood tide, (2) after the peak of the flood tide, and (3) at the lowest point of the ebb tide. Salinity (YSI 30 probe) was measured in situ. Tidal data at the SAR outlet was generated using WXtide software (FlaterCo). Samples for optical analysis were immediately filtered using 0.7-$\mu$m glass-fiber filters (Whatman Inc.) and stored in amber glass bottles (Qorpak, VWR) in the dark at 4°C until analysis in the laboratory. Before optical analysis, the samples were warmed to room temperature.

*Optical properties*—Absorbance spectra were measured with a diode-array ultraviolet (UV)-visible spectrometer (Agilent Technologies 8453) from 200 to 700 nm in a quartz sample cell (path length = 10 cm) with a deionized water blank. Absorbance was transformed to absorption coefficient (m$^{-1}$) by multiplying the measured absorbance at 300 nm by 2.303 and dividing by the path length in meters (Hu et al. 2002); 300 nm is a wavelength commonly reported for CDOM absorbance for intercomparisons (Miller 1998). Spectral slopes (*S*) were calculated by fitting the spectral data to Eq. (2) with a first-order linear regression for 300–400 nm:

$$\text{Abs} = A_0 \exp[-S(\lambda - \lambda_0)] \qquad (1)$$

$$-S = [(\ln \text{Abs}/A_0)/\lambda - \lambda_0)] \qquad (2)$$

where Abs is the absorbance (m$^{-1}$) at wavelength $\lambda$ and $A_0$ is the absorbance at reference wavelength $\lambda_0$ (Green and Blough 1994; Warnock et al. 1999; Moran et al. 2000). For all *S* calculations, $R > 0.999$ with $p < 0.0001$.

Emission spectra were obtained with a scanning fluorometer (Quantamaster, PTI). 3D excitation–emission matrix fluorescence spectra (EEMs) were obtained by ranging the excitation wavelengths from 260 to 455 nm and the emission wavelengths from 270 to 705 nm in 5-nm increments. A water EEM was generated daily to subtract out the water Raman peak (from a Whatman Nanopure ion exchanger), and spectra were corrected for instrumental response. Percentage error on three duplicate absorbance and fluorescence scans was <0.5%.

*Residence time mixing model*—The residence time of water in the sloughs was estimated using the following analysis that specifically takes into account mixed tides and fortnightly changes in tidal amplitude. Consider a conservative tracer (e.g., a nonreacting dye) that is instantaneously and completely mixed into the slough at the beginning of an ebb tide. Because the dye does not undergo reaction, its concentration in the slough does not change until the beginning of the next flood tide, when it is diluted by clean (i.e., dye-free) ocean water, assuming that none of the dye from the previous ebb is reentrained on the flood. At the end of the first flood tide, the relative concentration (or volume fraction) of dye in the slough is given by the ratio $C_1 = (V_{LT}/V_{HT})_1$ (Fisher et al., 1979), where $V_{LT}$ and $V_{HT}$ represent the volume of water in the slough at the low-tide and high-tide mark, respectively. Over a sequence of $k$ flood tides (each characterized by their own low- and high-tide volumes), the relative concentration of dye in the slough declines according to the equation

$$C_k = \prod_{n=1}^{k} \left(\frac{V_{LT}}{V_{HT}}\right)_n \qquad (3)$$

where the symbol $\Pi$ denotes a sequence of multiplications. An average residence time can be associated with this dilution sequence by assuming that the concentration of dye in the slough decays exponentially with time:

$$C(t_k) = \exp(-t_k/T_f) \qquad (4)$$

where $t_k$ is the elapsed time between the introduction of the dye (at $t_k = 0$) and the end of the $k$th flood tide and $T_f$ represents an empirical flushing time constant, sometimes called the estuarine residence time (Sheldon and Alber 2006). Physically, the parameter $T_f$ represents the time it takes to flush a given fraction (in this case 1/e) of a conservative tracer from the slough. $T_f$ was estimated for the two sloughs studied here by computing $V_{LT}$ and $V_{HT}$ for each flood–ebb tide cycle using measured tide levels and digital elevation maps for the sloughs (provided courtesy of B. Sanders, University of California, Irvine). These calculations were carried out for the sequence of flood tides that occurred coincident with the collection of water samples for CDOM measurements (26 June 2001–17 July 2001). Equation 3 was then fit to the sequence of $C_k$ values obtained from Eq. 4 to yield estimates (and standard deviations) for $T_f$.

*Photodegradation experiments*—Common plants growing at the salt marsh sites were collected to examine the optical properties and photodegradation of CDOM produced. Specimens collected were saltbush (*Atriplex lentiformis*), pickleweed (*Salicornia virginica*), sea fig (*Carpobrotus chilensis*), saltwort (*Batis maritima*), alkali health (*Frankenia grandiflora*), and brown seaweed (*Macrocystis pyrifera*, growing on the tide gates) (Yale-Dawson and Foster 1982; Rundel and Gustafson 2005). Senescent plant samples were washed with deionized water and placed in 2.0-liter glass flasks containing a 0.1% sodium azide (NaN$_3$) solution (Fisher Scientific) to kill bacteria. The addition of NaN$_3$ has been shown to initiate the formation of color and polymerization reactions (Scully et al. 2004). We monitored the rate of fluorescence decay on specific EEM peaks from the initial solution, which should not be affected. Solutions were made up in artificial seawater (aqueous NaCl solution; salinity 33) to mimic the marsh environment. Flasks were placed in the dark at 22°C for 24 h to dissolve optically active material formed in the senescent plants and filtered under a gentle vacuum through 0.7-$\mu$m glass-fiber filters to remove large particulate material (Whatman). Six plant leachate irradiation samples, dark controls covered with aluminum foil, and a 0.1% NaN$_3$ solution control were placed in direct sun from

Table 1. Tide height (m), salinity (sal.), and absorption coefficient at 300 nm (abs; m$^{-1}$) by tidal stage for stations W2, W4, and W5.

| Site | Date | Preflood | | | | Postflood | | | | Ebb | | | |
|------|------|------|----------|------|----------------|------|----------|------|----------------|------|----------|------|----------------|
| | | Time | Tide (m) | Sal. | Abs. (m$^{-1}$) | Time | Tide (m) | Sal. | Abs. (m$^{-1}$) | Time | Tide (m) | Sal | Abs. (m$^{-1}$) |
| W2 | 26 Jun | 00:00 | 1.49 | 31.8 | 2.7 | 03:00 | 1.29 | 31.8 | 1.9 | 07:00 | 0.040 | 32.3 | 2.2 |
| W4 | | | | 32.0 | 4.4 | | | 31.9 | 2.0 | | | 31.8 | 3.8 |
| W5 | | | | 32.0 | 3.2 | | | 31.9 | 2.3 | | | 31.9 | 4.4 |
| W2 | 28 Jun | 02:00 | 1.05 | 31.6 | 7.1 | 05:00 | 1.10 | 31.6 | 1.3 | 09:00 | 0.28 | 30.6 | 3.5 |
| W4 | | | | 32.1 | 3.9 | | | 31.9 | 2.0 | | | 32.1 | 4.7 |
| W5 | | | | 32.0 | 9.0 | | | 32.2 | 2.6 | | | 32.4 | 8.0 |
| W2 | 04 Jul | 20:00 | 1.76 | 31.8 | 7.1 | 23:00 | 1.48 | 31.7 | 1.5 | 03:00 | −0.037 | 32.4 | 3.0 |
| W4 | | | | 32.0 | 6.2 | | | 32.2 | 4.7 | | | 31.8 | 3.8 |
| W5 | | | | 32.1 | 5.9 | | | 31.9 | 3.2 | | | 32.1 | 4.2 |
| W2 | 08–09 Jul | 22:00 | 1.50 | 31.9 | 3.8 | 01:00 | 1.38 | 31.7 | 2.0 | 06:00 | 0.037 | 30.8 | 5.5 |
| W4 | | | | 31.9 | 4.4 | | | 32.5 | 2.3 | | | 32.1 | 5.4 |
| W5 | | | | 31.6 | 3.3 | | | 31.9 | 2.3 | | | 32.0 | 5.3 |
| W2 | 12 Jul | 00:00 | 1.10 | 31.7 | 6.2 | 03:00 | 1.07 | 31.5 | 2.3 | 08:00 | 0.34 | 30.4 | 5.1 |
| W4 | | | | 31.6 | 3.6 | | | 31.6 | 2.4 | | | 31.9 | 3.8 |
| W5 | | | | 31.9 | 7.6 | | | 31.7 | 4.3 | | | 32.6 | 6.5 |
| W2 | 20–21 Jul | 22:00 | 1.88 | 31.7 | 1.3 | 23:00 | 1.80 | 31.9 | 1.3 | 04:00 | −0.36 | 31.3 | 2.3 |
| W4 | | | | 31.8 | 2.0 | | | 31.7 | 1.2 | | | 32.0 | 2.7 |
| W5* | | | | — | — | | | 31.8 | 1.5 | | | 32.2 | 3.7 |

* The data for station W5, 20 Jul 2001, ebb tide, are not recorded, as this sample was broken during storage.

09:30 to 17:30 h local time 05 June 2002 on the roof of the Hashinger Science building (Chapman University, Orange, California); sunrise occurred at 05:41 h and sunset at 20:00 h. Precautions were taken to avoid self-shading. Twenty-milliliter aliquots were collected at time intervals of 0, 1, 2, 4, 6, and 8 h and stored briefly in the dark at 4°C until optical analyses could be performed (UV-visible, <2 h; fluorescence, <8 h).

## Results

The tide height, salinity, and absorption coefficient at 300 nm are shown in Table 1 for all three sites. Six tidal cycles were sampled in total, with three samples taken at each site per tidal cycle: before the peak of the flood tide (preflood), after the peak of the flood tide (postflood), and at the lowest point of the ebb tide (ebb). The measured range in salinity over all samples was 31–33, consistent with a saline tidally flushed salt marsh environment. At site W2, the salinity decreased slightly to 30.5 during some ebb tides (three of six sampled), even though saline water was ebbing from the salt marshes. This is likely due to additional freshwater inputs from urban runoff from a storm-water drain located ~3.5 m downstream from site W2 (*see* Fig. 1).

Absorption coefficients at 300 nm (in m$^{-1}$) are reported in Table 1. Absorbance spectra were characteristic for CDOM, exhibiting a decrease in absorbance with increasing wavelength (Del Vecchio and Blough 2004). Average absorption coefficients doubled at ebb vs. flood tides (4.8 ± 1.5 vs. 2.1 ± 0.9 m$^{-1}$), when there was no dilution by inflowing ocean water, suggesting significant salt marsh CDOM inputs into the river outlet and thence into the coastal waters. Absorption coefficients at postflood and ebb tides were generally higher for the slough sites W4 and

W5 than the SAR site W2, again suggesting an input of CDOM from the salt marshes.

Covariance analyses of UV and visible wavelengths have been used to differentiate between sources of CDOM and between freshly produced or degraded material (Miller 1998). A plot of the absorption coefficient at 300 nm vs. the absorption coefficient at 254 nm for all three sites for all ebb, preflood, and postflood tidal cycles is linear (Fig. 2), indicating a single source of CDOM diluting out. This suggests that the salt marshes are the dominant sources of terrestrial CDOM to these coastal waters in the dry season in the absence of riverine inputs. The outlier labeled on Fig. 2 occurred at station W2 during an offshore upwelling cold-water event and indicates a second source of marine CDOM, most likely from bacterial production from marine phytoplankton exudates (McKnight and Aiken 1998). A phytoplankton bloom was observed at coastal sites over this sampling period in a related study (Grant et al. 2002).

Spectral slopes are another tool in differentiating between the sources and bleaching extent of organic matter in aquatic systems (Green and Blough 1994; De Souza Sierra et al. 1997; Seritti et al. 1998). In a recent study (Tzortziou et al. 2007), different spectral slopes for CDOM from a tidal marsh vs. an adjacent river estuary were attributed to marsh-derived CDOM with distinct optical and chemical composition. Our *S* values ranged from 0.0100 to 0.0112 nm$^{-1}$ with no statistical difference between ebb vs. flood tides and sites, consistent with a single source of similarly bleached CDOM in the marsh and surf zone waters. Our *S* values are on the low end of the range (0.012–0.018 nm$^{-1}$) previously reported for estuarine waters (Vodacek et al. 1997; Stabenau et al. 2004; Tzortziou et al. 2007). Lower *S* values have been attributed to a CDOM fraction that is more humic or more terrestrial in nature (Green and Blough 1994; Vodacek
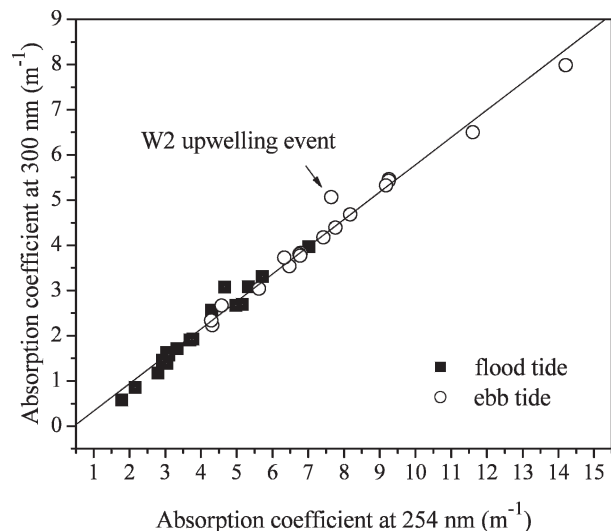
Fig. 2. Absorption coefficient (at 300 nm; $m^{-1}$) vs. absorption coefficient (at 254 nm; $m^{-1}$) for ebb, preflood and postflood cycles for all three sites. The upwelling cold-water event sampled at station W2 at flood tide at 05:00 h on 28 June 2001 is noted. Line shown from fit to a first-order linear regression, $R = 0.99$, $p < 0.0001$.

et al. 1997; Whitehead et al. 2000). *S* values increase as CDOM is photobleached and decrease with aging in soils and sediments (Stabenau et al. 2004; Tzortziou et al. 2007). The *S* values measured here suggest a higher-molecular-weight, aged CDOM source with more terrestrial-like humic character. Hence, the low *S* values may be due to material from sediment pore waters dominating export of CDOM that has undergone aging and/or formation of higher-molecular-weight material in the marsh sediments.

3D EEMs have previously been shown to distinguish between CDOM sources in natural waters (Coble 1996; De Souza Sierra et al. 1997; McKnight et al. 2001). Peak locations and classifications used in this study were based on Coble's (1996) work, where five main fluorescent peaks were identified with distinct excitation and emission wavelength regions: (1) peak B, tyrosine protein-like (maximum excitation wavelength [$Ex_{max}$]: maximum emission wavelength [$Em_{max}$] 275/310 nm); (2) peak T, tryptophan protein-like ($Ex_{max}/Em_{max}$ 275/340 nm); (3) peak A, humic-like ($Ex_{max}/Em_{max}$ 260/380–460 nm); (4) peak M, marine humic-like $Ex_{max}/Em_{max}$ 312/380–420 nm); and (5) peak C, terrestrial humic-like ($Ex_{max}/Em_{max}$ 350/420–480 nm). The humic peaks A and C are present in waters containing terrestrially derived CDOM, whereas the protein peaks B and T are observed in freshly produced material. The marine peak M is characteristic of marine CDOM produced in the ocean by phytoplankton and microbial processes (Coble 1996).

Typical 3D EEM spectra for the salt marsh outlets are shown in Fig. 3 for flood and ebb tides; the same spectra are shown as contour plots in Fig. 4. The protein peak T was observed in all slough samples at ebb tide, indicating freshly produced material flowing out of the salt marshes. The Lower Slough site W4 consistently had a strong protein peak at flood tide but low terrestrial humic peaks (Fig. 4). Since

this strong protein-like peak is not observed at Upper Slough site W5 on the flood tide, a direct source of proteinaceous material at site W4 accessible at flood tide is the most likely cause, possibly the sea-fig plants that grow on the bank by the tide gate and are submerged at flood tide.

During ebb tide for the slough sites W4 and W5, humic peaks A and C are present, indicating waters containing terrestrially derived CDOM; peak C is elongated, a typical feature of natural CDOM due to the presence of multiple fluorophores. As expected during the flood tide, the terrestrial humic signals (peaks A and C) are lower in the incoming surf-zone water because of the dilution of high-CDOM inputs by low-CDOM ocean water. This has been seen in previous studies where the terrestrial humic peak is decreased when mixed with seawater because of simple dilution (Coble 1996; Seritti et al. 1998). The Upper Slough site W5 had an additional peak with marine humic-like characteristics (M; Fig. 4), indicating production of marine humic-like material by salt marshes. From 28 June to 01 July 2001, ocean temperatures dropped, and an intense marine CDOM signal was observed at the SAR outlet (site W2) on a postflood tide (Fig. 5).

To examine the optical characteristics of CDOM produced from salt marsh plants, EEMs were obtained of leachates from three salt marsh plants, *Salicornia virginica* (pickleweed), *Batis maritimia* (saltwort), and *Frankenia grandiflora* (alkali health) (Yale-Dawson and Foster 1982). Additional species growing in the sloughs were *Atriplex lentiformis* (salt bush), typically found on coastal bluffs and terraces (Rundel and Gustafson 2005), and *Macrocystis pyrifera* (brown seaweed) growing on the tide gate at site W4. *Carpobotus chilensis* (sea fig) was exclusive to the more anthropogenically affected Lower Slough (W4).

Peak positions pre- and postirradiation, peak classifications, and maximum preirradiation fluorescent intensities are shown in Table 2; five protein peaks and three marine and three terrestrial humic-like peak contributions were observed from these six plant species. The EEMs showed that two species of plants (sea fig, saltwort) produced fluorescent materials dominated by protein-like peaks with no accompanying humic peaks (Fig. 6). The same EEMs are shown as contour plots in Fig. 7. The brown seaweed growing on the tide gates produced a terrestrial humic-like peak in addition to the protein peak. Unexpectedly, the remaining three plant species produced marine humic-like peaks.

The residence time scales calculated for the sloughs were $12.8 \pm 0.1$ h for the Upper Slough and ~9% longer at $14.6 \pm 0.1$ h for the Lower Slough. To measure the extent of photodegradation on this time scale, the plant leachates were exposed to natural sunlight for 8 h from early morning to late afternoon, and the change in the EEM fluorescent peaks was monitored as a function of irradiation time. Spectral slopes for the leachates postirradiation averaged $0.016 \pm 0.02$ $nm^{-1}$, higher than measured for the salt marsh ebb samples. This suggests that the low spectral slope values for the ebbing salt marsh waters may be due to material from pore waters in the sediments dominating CDOM export, with lower spectral slopes associated with aging and/or formation of higher-molecular-weight material in the marsh sediments.
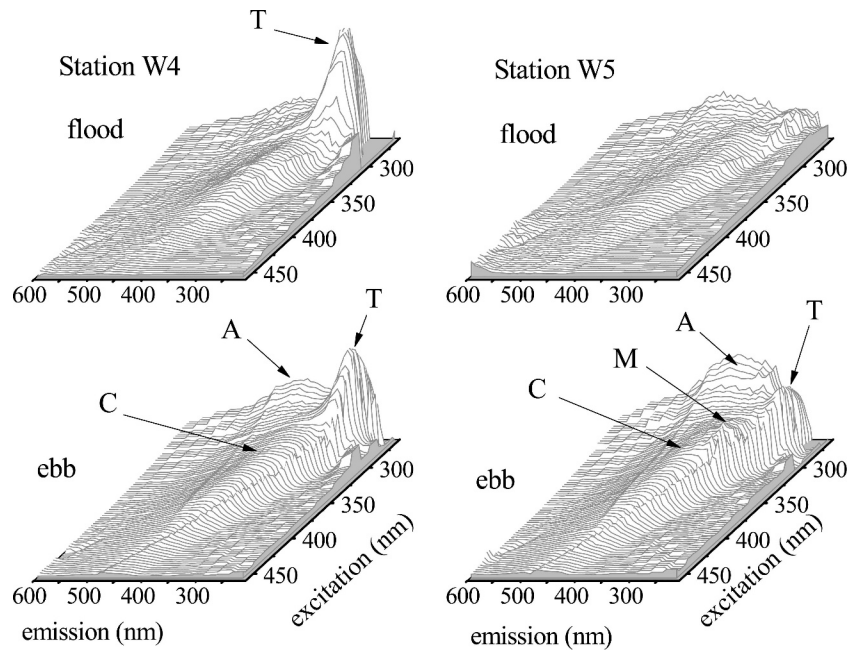
Fig. 3. Representative 3D-EEMS and corresponding contour plots for flood and ebb tide at the salt marsh sites W4 and W5. The protein (T), terrestrial humic (A and C), and marine humic peaks (M) are labeled. Plots are normalized to the same maximum fluorescence intensity of $3.6 \times 10^4$ counts s$^{-1}$ on the z-axis.
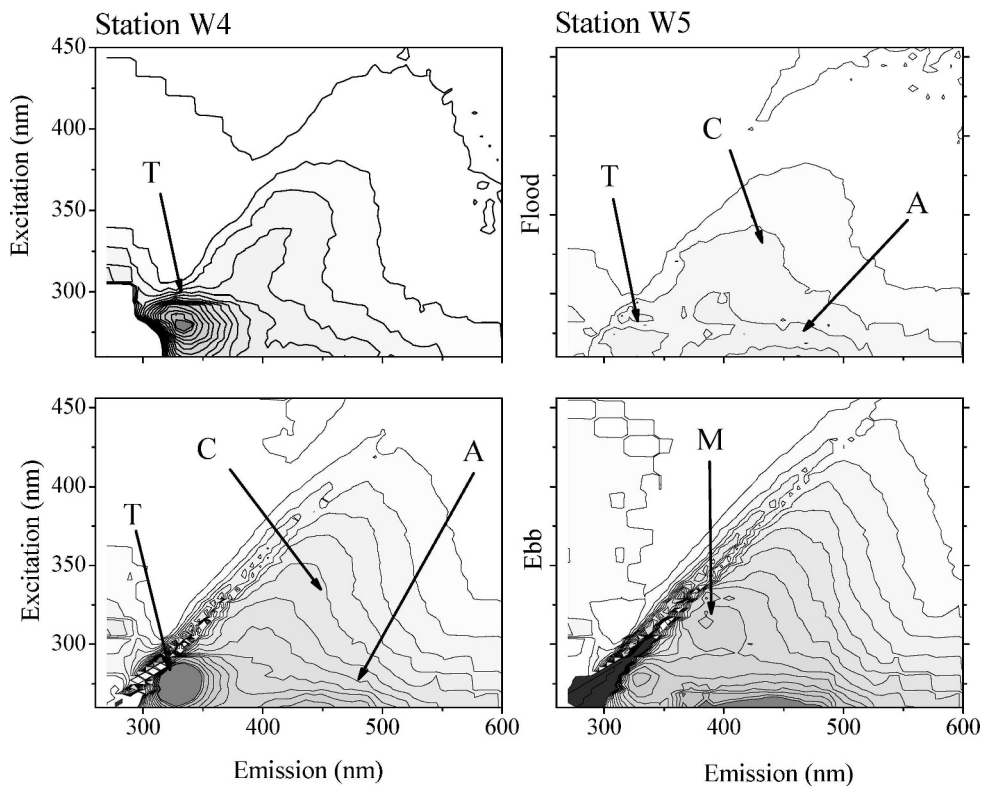


Fig. 4. The same EEMS as in Figure 3 are shown as contour plots. Contour lines are shaded on the basis of increasing fluorescence intensity from white (0) to dark gray ($3.6 \times 10^4$ counts s$^{-1}$).
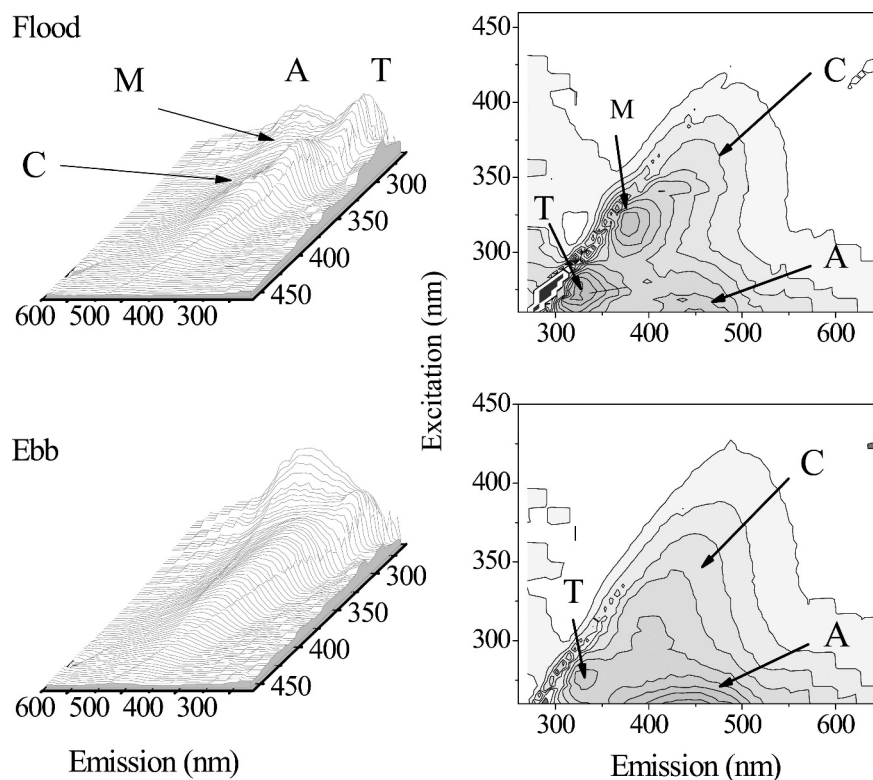
Fig. 5. 3D EEMs taken during the cold-water upwelling event on 28 June 2001 for the river mouth site W2. Postflood: 05:00 h; ebb: 09:00 h. The protein (T), terrestrial humic (A and C), and marine humic peaks (M) are labeled. Plots are normalized to the same maximum fluorescence intensity of $3.6 \times 10^4$ counts s$^{-1}$ on the z-axis. The EEMS are also shown as contour plots on the RHS. Contour lines are shaded on the basis of increasing fluorescence intensity from white (0) to dark gray ($3.6 \times 10^4$ counts s$^{-1}$).

For the proteinaceous peak, most plant species were resistant to degradation. However, the saltwort protein peak increased with irradiation time, and the sea-fig protein peak decayed rapidly with solar irradiation (Fig. 8), with a significant blue shift in the T peak emission maximum for this species only (Table 2). This variability might be due to the rapid transformation of photochemically active polyphenols, as previously shown for mangrove plant leachates (Scully et al. 2004); polyphenols have similar fluorescence characteristics to the T and B peaks. The marine (M) and

Table 2. Peak positions pre- and postirradiation (excitation and emission maximum wavelength; Ex$_{max}$/Em$_{max}$), peak classifications, maximum preirradiation fluorescent intensities (flu. int.), first-order decay rate constants ($k$), kinetic fit regression coefficients ($R$), and half-lives (h) for the salt marsh plant leachates.

| Salt marsh plant | Ex$_{max}$/Em$_{max}$ preirradiation (nm) | Ex$_{max}$/Em$_{max}$ postirradiation (nm) | Peak type* | Flu. int. ($\times 10^5$ counts s$^{-1}$) | $k$ ($\times 10^{-5}$ s$^{-1}$) | $R$† | Half-life (h) |
|---|---|---|---|---|---|---|---|
| *Atriplex lentiformis* (saltbush) | 274/334 | 275/331 | T | 11.1 | — | — | — |
| | 314/436 | 315/433 | M | 7.01 | 2.2±0.4 | 0.93 | 9±2 |
| *Salicornia virginica* (pickleweed) | 311/436 | 310/432 | M | 15.1 | 1.4±0.1 | 0.99 | 14±1 |
| | 274/333 | 275/337 | T | 5.56 | — | — | — |
| *Carpobrotus chilensis* (sea fig) | 274/327 | 275/305 | T/B | 9.79 | 3.0±0.4 | 0.97 | 6±1 |
| *Batis maritima* (saltwort) | 271/301 | 270/300 | B | 24.9 | −5±2 | 0.84 | −3.8±1.2‡ |
| *Frankenia grandiflora* (alkali health) | 306/423 | 300/414 | M | 6.35 | 1.1±0.3 | 0.85 | 18±5 |
| *Macrocystis pyrifera* (brown seaweed) | 271/304 | 270/304 | B | 1.37 | — | — | — |
| | 274/442 | 270/444 | A | 1.03 | 1.3±0.4 | 0.84 | 15±5 |
| | 343/449 | 345/445 | C | 1.03 | 1.0±0.4 | 0.74 | 20±9 |

* T, tryptophan, and B, tyrosine-like protein peaks; A and C, terrestrial humic-like peak; M, marine humic-like (Coble 1996).
† Data shown only for statistically significant first-order decay fits with $p < 0.1$.
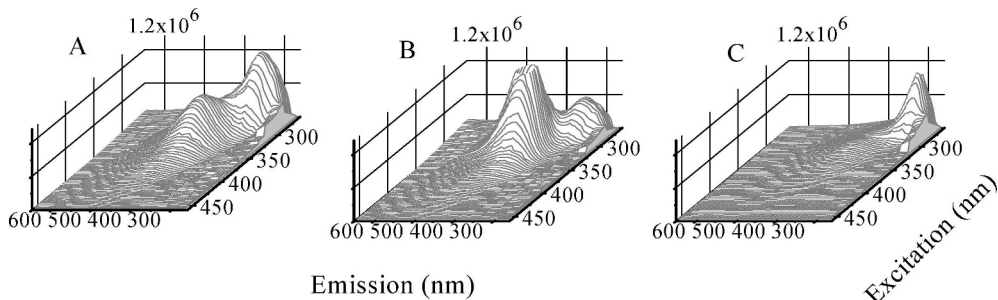‡ This is for the peak growth.

Fig. 6. EEMs for the salt marsh plant leachates before irradiation. All EEMs are shown on the same maximum fluorescence intensity scale of $1 \times 10^6$ counts s$^{-1}$ on the z-axis for ease of comparison, except for D (higher at $2.0 \times 10^6$ counts s$^{-1}$) and F (lower at $1.0 \times 10^5$ counts s$^{-1}$) to better show peak details.

terrestrial (A and C) humic-like peaks all decreased in fluorescence intensity with time (Fig. 9), with the M peak emission maximum undergoing a small blue shift and the A peak a small red shift after 8 h of irradiation; that is, essentially the same materials are present after irradiation but at lower levels.

## Discussion

The increase of the absorption coefficients at ebb vs. flood tides suggests that salt marshes are a significant source of CDOM to coastal waters. The linear covariance plot and similar $S$ values for all the ebb and floodwaters sampled at all
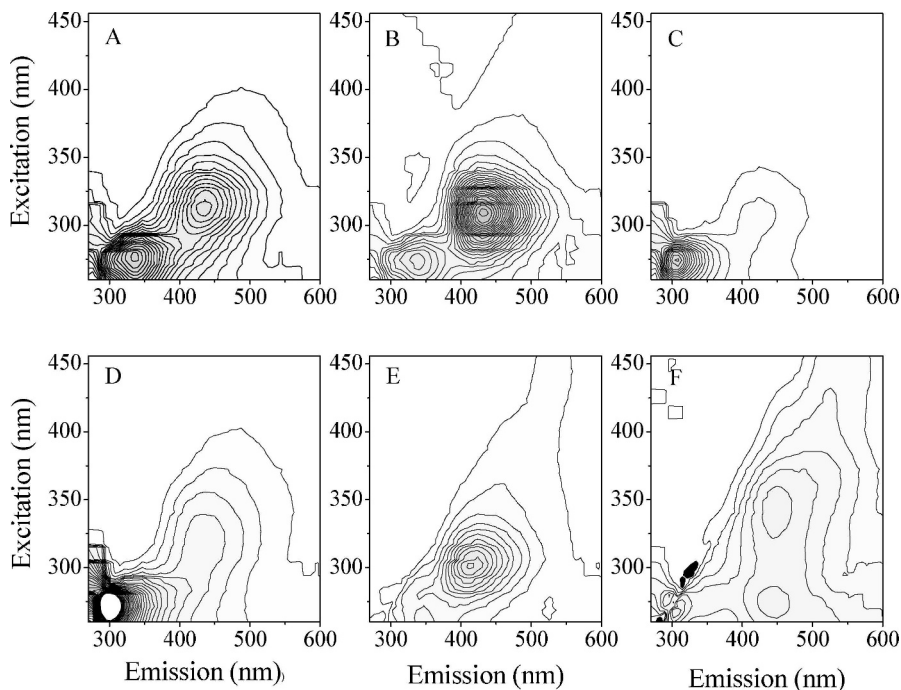


Fig. 7. The same EEMs as shown in Figure 6 are shown as contour plots. Contour lines are shaded on the basis of increasing fluorescence intensity from white (0) to dark grey ($3.6 \times 10^4$ counts s$^{-1}$).
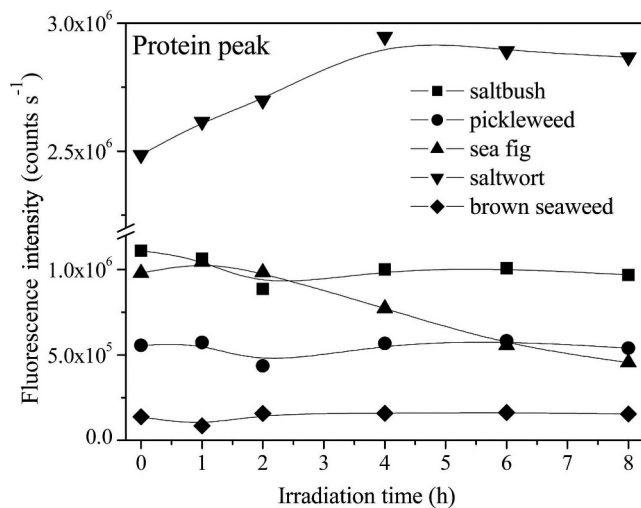
Fig. 8. Fluorescence intensity (counts s$^{-1}$) vs. solar irradiation time (h) for the protein peaks in the salt marsh plant leachates.



Fig. 9. Fluorescence intensity (counts s$^{-1}$) vs. solar irradiation time (h) for the humic peaks in the salt marsh plant leachates. M, marine humic; A and C, terrestrial humics.

sites suggests that this exported salt marsh CDOM dominates nearshore waters in the absence of rainfall in the dry season. An additional CDOM end member based on optical properties was measured in flooding waters during a single offshore upwelling event and attributed to a marine source based on the outlier on the covariance analysis plot (Fig. 2), the presence of a strong M humic-like peak, and an increased protein peak (Fig. 5) compared to other flooding coastal waters at the same site that suggested active marine production at this time.

Autochonthous sources have been shown to contribute to DOM production in treatment wetlands in California, with the nature of the DOM produced governed by vegetation patterns (Barber et al. 2001). A previous study associated lignin with the production of a large fraction of humic substances in coastal wetlands (Moran and Hodson 1994), whereas intertidal vascular plants dominate fluorescent DOM production in mangroves (Moran et al. 1991). Production of marsh or mangrove DOM with distinctive fluorescent properties has been previously shown (Gardner et al. 2005; Maie et al. 2006). In our study, marine and terrestrial humic-like peaks and protein peaks were observed for leachates of common salt marsh plants. Protein-like peaks are expected for freshly produced degraded plant material, but these peaks may also be due to polyphenols, which have similar fluorescence characteristics to the T protein peak and are also produced by freshly degraded plant material (Scully et al. 2004).

Sea fig and saltwort produced only protein-like peaks, with elevated levels at one site at flood tide attributed to sea-fig plants growing nearby. Unexpectedly, a protein-like peak and terrestrial humic-like peaks were produced by the brown seaweed growing on the tide gates. Submerged seagrass beds in coastal South Florida have previously been shown to be significant contributors of CDOM with terrestrial characteristics to coastal waters (Stabenau et al. 2004), making up 40–50% of the coastal CDOM pool. There is no seagrass offshore at this site, but it does occur in parts of the down coast Upper Newport Back Bay (Pednekar et al. 2005).
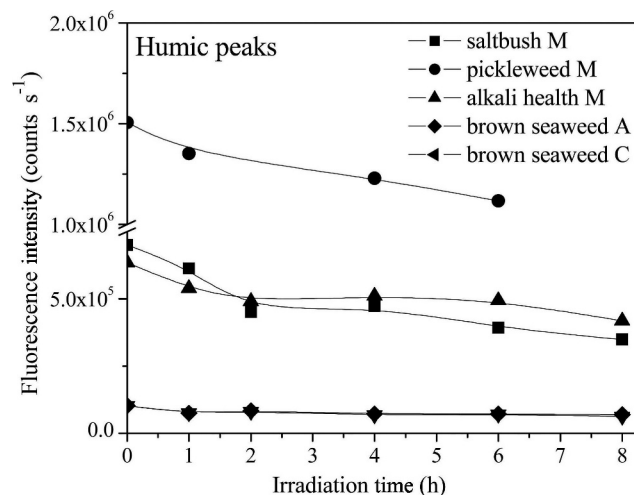
Three of the salt marsh species produced marine humic-like peaks in addition to protein peaks, specifically saltbush, pickleweed, and alkali health. Stedmon and Markager (2005) also reported the unusual production of a marine humic-like peak in a freshwater stream impacted by agricultural waste. The M peak was observed in natural waters in this study only at ebb tides at site W5, suggesting CDOM production from the abundant pickleweed and saltbush in the Upper Slough. However, this marine humic-like peak was not observed in the coastal waters in the flood samples (except for the offshore source during the upwelling event), suggesting that it must be rapidly photodegraded and/or biologically utilized after export from the marsh. Although it appears to be rapidly utilized in coastal waters, it is important to note that salt marsh plants produce material with marine humic-like CDOM signals and that salt marshes may be an overlooked but important source of marine humic-like material in coastal waters.

Although the senescent salt marsh plants sampled produced protein and humic-like fluorescent peaks on submersion in water, whether all these optically active materials will enter the coastal ocean depends on residence times in the sloughs and the rate of photochemical and biological degradation processes. The calculated residence times of 12–15 h for the sloughs are comparable to the times expected for tidal flushing based on the semidiurnal tidal cycle, with two flood and two ebb tides per 24-h period (Noblet et al. 2004). This makes sense, as the sloughs drain almost completely on an ebb tide. Photodegradation data from 8-h solar irradiations were fit to pseudo–first-order kinetics by plotting ln (initial fluorescence intensity ÷ fluorescence intensity) vs. time (s) for the decay of the fluorescence of the salt marsh plant leachate peaks with solar irradiation. The rate constants and half-lives are shown in Table 2 for the seven plant leachate peaks that had statistically significant first-order decay fits ($p < 0.1$). There was no statistically significant decay in the dark controls. The half-life was shortest at $6 \pm 1$ h for the sea-fig

protein peak; by contrast, the saltwort protein peak had a half-life of $-3.8 \pm 1.2$ h.

The remaining species had protein peaks resistant to photodegradation over the course of this study. Since the protein peak is weak in the Upper Slough W5 ebb samples compared to the humic-like peaks, this protein material must undergo rapid biological decay pathways in the salt marsh as previously shown for wetland-derived DOM (Scully et al. 2004). For the salt marsh marine humic-like peaks (M), half-lives ranged from $9 \pm 2$ h for the saltbush to $18 \pm 5$ h for the alkali health species. The terrestrial humic-like peaks (A and C) of the brown seaweed had a half-life of $15 \pm 5$ h. Half-lives over all degraded humic peaks averaged $15 \pm 5$ h, within the range observed for all species. This is on the order of the residence time for the sloughs. In a recent study of the photobleaching of CDOM from seagrass leachates, the half-life for absorbance loss ranged from 20 to 30 h depending on temperature, with the fluorescence decay of the humic peak reported as being faster (Stabenau et al. 2004). Half-lives of 18–27 h have been reported for mangrove and wetland leachates' fluorescence decay by photochemical degradation (Scully et al. 2004).

Our studies were conducted in the absence of microbial and other biological decay pathways, which have previously been shown to be much slower than photochemical decay for plant-derived DOM from mangroves and wetlands (Scully et al. 2004). However, photodegraded salt marsh CDOM has been shown to be more biologically available (Miller and Moran 1997). The measured photochemical half-lives on the order of the slough residence times measured here thus have implications for the biological availability and cycling of marsh-derived DOM in coastal waters. Based on the calculated half-lives, around 40–60% of the CDOM produced by salt marsh plants would be exported unbleached to the surf zone in a tidal cycle in the absence of biological cycling.

The lower spectral slopes and reduced protein peaks measured in the marsh ebb waters vs. the leachates, coupled with the rapid photodegradation of plant leachate humic materials over the short marsh residence times, suggest that higher-molecular-weight, more aged, and/or more terrestrial humic-like CDOM is exported from the salt marshes than would be predicted from the freshly formed plant leachates. This suggests that pore waters in marsh sediments are likely the major source of exported marsh DOM, with a minor contribution from fresh plant materials. Previous studies have shown that mangrove pore waters are a major source of CDOM to adjacent estuaries (Tremblay et al. 2007).

Southern California gets ~15 cm of rain a year on average over the wet season in January–February, when river inputs increase for a few days following a rainfall. For the rest of the year, river mouths operate as tidally flushed systems (Grant et al. 2005). There are usually only about three to four freshwater flow events per wet season, whereas the salt marshes would be a largely constant CDOM source throughout the year. Since Southern California experiences no river flow for 99% of the year, salt marshes should dominate the coastal water CDOM inputs both temporally and quantitatively, particularly if the sediments, rather than seasonally varying senescent plant sources, are the major exporters of CDOM.

In conclusion, the results of this study suggest that salt marshes are significant exporters of CDOM and should be the dominant CDOM source in coastal waters in dry regions. Common salt marsh plant species were found to rapidly produce protein-like and humic-like fluorescent material, with three species producing material with marine humic-like properties. Thus, salt marshes can produce and export marine humic-like material to coastal waters. This material may be rapidly photodegraded and/or biologically utilized in coastal waters, as it was not present in flood tide samples in the absence of the upwelling event. Humic peak stabilities to photochemical decay were on the order of the residence time in the marshes, suggesting that about half the CDOM from salt marsh plants would be exported to coastal waters in the absence of biological processing. Salt marshes are an understudied but potentially major contributor to CDOM dynamics in coastal areas and the coastal carbon pool, particularly in regions with little to no rainfall and freshwater inputs.

## References

BARBER, L. B., J. A. LEENHEER, T. I. NOYES, AND E. A. STILES. 2001. Nature and transformation of dissolved organic matter in treatment wetlands. Environ. Sci. Technol. **35:** 4805–4816, doi:10.1021/es10518i.

BOYD, T. J., AND C. L. OSBURN. 2004. Changes in CDOM fluorescence from allochthonous and autochthonous sources during tidal mixing and bacterial degradation in two coastal estuaries. Mar. Chem. **89:** 189–210, doi:10.1016/j.marche.2004.02.012.

CLARK, C. D., J. JIMENEZ-MORAIS, G. JONES, E. ZANARDI-LAMARDO, C. A. MOORE, AND R. G. ZIKA. 2002. A time-resolved fluorsecence study of dissolved organic matter in a riverine to marine transition zone. Mar. Chem. **78:** 121–135.

COBLE, P. G. 1996. Characterization of marine and terrestrial DOM in seawater using excitation-emission matrix spectroscopy. Mar. Chem. **51:** 325–346.

DEL VECCHIO, R., AND N. V. BLOUGH. 2004. On the origin of the optical properties of humic substances. Environ. Sci. Technol. **38:** 3885–3891.

DE SOUZA SIERRA, M. M., O. F. X. DONARD, AND M. LAMOTTE. 1997. Spectra identification and behavior of dissolved organic fluorescent material during estuarine mixing processes. Mar. Chem. **58:** 51–58.

DITTMAR, T., N. HERTKORN, G. KATTNER, AND R. J. LARA. 2006. Mangroves, a major source of dissolved organic carbon to the oceans. Glob. Biogeogr. Cycles **20:** GB1012, doi:10.1029/2005GB002570.

FISHER, H. B., E. J. LIST, R. C. Y. KOH, J. IMBERGER, AND N. H. BROOKS. 1979. Mixing in inland and coastal waters. Academic Press.

GALLEGOS, C. L., T. E. JORDAN, A. H. HINES, AND D. E. WELLER. 2005. Temporal variability of optical properties in a shallow, eutrophic estuary: Seasonal and interannual variability. Estuar. Coast. Shelf Sci. **64:** 156–170.

GARDNER, G. B., R. F. CHEN, AND A. BERRY. 2005. High-resolution measurements of chromophoric dissolved organic matter (CDOM) in the Neponset River Estuary, Boston Harbor, MA. Mar. Chem. **96:** 137–154, doi:10.1016/j.marchem.2004.12.006.

GRANT, S. B., J. H. KIM, B. H. JONES, S. A. JENKINS, J. WASYL, AND C. CUDABACK. 2005. Surf-zone entrainment, along-shore transport and human health implications of pollution from tidal outlets. J. Geophys. Res. **110:** C10025, doi:10.1029/2004JC002401.

———, AND OTHERS. 2002. Coastal run-off impact study phase II: Sources and dynamics of fecal indicators in the lower Santa Ana River watershed. Technical report, National Water Research Institute.

GREEN, S. A., AND N. V. BLOUGH. 1994. Optical absorption and fluorescence properties of chromophoric dissolved organic matter in natural waters. Limnol. Oceanogr. **39:** 1903–1916.

HESSEN, D. O., AND L. J. TRANVIK. 1998. Aquatic humic matter: From molecular structure to ecosystem stability, p. 333–343. *In* D. O. Hessen and I. J. Tranvik [eds.], Ecological studies: Aquatic humic substances. Springer-Verlag.

HU, C., F. E. MULLER-KARGER, AND R. G. ZEPP. 2002. Absorbance, absorption coefficient and apparent quantum yield: A comment on common ambiguity in the use of these optical concepts. Limnol. Oceanogr. **47:** 1261–1267.

MAIE, N., J. N. BOYER, C. Y. YANG, AND R. JAFFE. 2006. Spatial, geomorphological and seasonal variability of CDOM in estuaries of the Florida Coastal Everglades. Hydrobiologia **569:** 135–150.

McKNIGHT, D. M., AND G. R. AIKEN. 1998. Sources and age of aquatic humus, p. 9–40. *In* D. O. Hessen and L. J. Tranvik [eds.], Ecological studies: Aquatic humic substances. Springer-Verlag.

———, E. W. BOYER, P. K. WESTERHOFF, P. T. DORAN, T. KULBE, AND D. T. ANDERSEN. 2001. Spectrofluorometric character-ization of dissolved organic matter for indication of precursor organic material and toxicity. Limnol. Oceanogr. **46:** 38–48.

McLUSKY, D. S., AND M. ELLIOTT. 2004. The estuarine ecosystem: Ecology, threats and management, 3rd ed. Oxford University Press.

MILLER, W. L. 1998. Effects of UV radiation on aquatic humus: Photochemical principles and experimental considerations, p. 125–144. *In* D. O. Hessen and L. J. Tranvik [eds.], Ecological studies: Aquatic humic substances. Springer-Verlag.

———, AND M. A. MORAN. 1997. Interaction of photochemical and microbial processes in the degradation of refractory dissolved organic matter from a coastal marine environment. Limnol. Oceanogr. **42:** 1317–1324.

MITSCH, W. J., AND J. G. GOSSELINK. 2000. Wetlands, 3rd ed. Wiley.

MORAN, M. A., AND R. E. HODSON. 1994. Dissolved humic substances of vascular plant origin in a coastal marine environment. Limnol. Oceanogr. **39:** 762–771.

———, W. M. SHELDON, AND R. G. ZEPP. 2000. Carbon loss and optical property changes during long-term photochemical and biological degradation of estuarine dissolved organic matter. Limnol. Oceanogr. **45:** 1254–1264.

———, R. J. WICKS, AND R. E. HODSON. 1991. Export of dissolved organic matter from a mangrove swamp ecosystem—evidence from natural fluorescence, dissolved lignin phenols and secondary bacteria production. Mar. Ecol. Prog. Ser. **76:** 175–184.

NOBLET, J. A., D. L. YOUNG, E. Y. ZENG, AND S. ENSARI. 2004. Use of fecal steroids to infer the sources of fecal indicator bacteria in the lower Santa Ana River watershed, California: Sewage is an unlikely source. Environ. Sci. Technol. **38:** 6002–6008.

OBERNOSTERER, I., AND R. BENNER. 2004. Competition between biological and photochemical processes in the mineralization of dissolved organic carbon. Limnol. Oceanogr. **49:** 117–124.

PEDNEKAR, A. M., S. B. GRANT, Y. JEONG, Y. POON, AND C. OANCEA. 2005. Influence of climate change, tidal mixing and watershed urbanization on historical water quality in New-port Bay, a saltwater wetland and tidal embayment in Southern California. Environ. Sci. Technol. **39:** 9071–9082.

ROCHELLE-NEWALL, E. J., AND T. R. FISHER. 2002. Production of chromophoric dissolved organic matter fluorescence in marine and estuarine environments: An investigation into the role of phytoplankton. Mar. Chem. **77:** 7–21, doi:10.1016/S0304-4203(01)00072-x.

RUNDEL, P. W., AND R. GUSTAFSON. 2005. Introduction to the plant life of Southern California. California Natural History Guide Series, no. 85. University of California Press.

SCULLY, N. M., N. MAIE, S. K. DAILEY, J. N. BOYER, R. D. JONES, AND R. JAFFE. 2004. Early diagenesis of plant-derived dissolved organic matter along a wetland, mangrove, estuary ecotone. Limnol. Oceanogr. **49:** 1667–1678.

SERITTI, A., D. RUSSO, L. NANNICINI, AND R. DEL VECCHIO. 1998. DOC, absorption and fluorescence properties of estuarine and coastal waters of the Northern Tyrrhenian Sea. Chem. Spec. Bioavail. **10:** 95–106.

SHELDON, J. E., AND M. ALBER. 2006. The calculation of estuarine turnover times using freshwater fraction and tidal prism models: a critical evaluation. Estuar Coasts **29:** 133–146.

STABENAU, E. R., R. G. ZEPP, E. BARTELS, AND R. G. ZIKA. 2004. Role of the seagrass *Thalassia testudinum* as a source of chromophoric dissolved organic matter in coastal South Florida. Mar. Ecol. Prog. Ser. **282:** 59–72.

STEDMON, C. A., AND S. MARKAGER. 2005. Resolving the variability in dissolved organic matter fluorescence in a temperate estuary and its catchment using PARAFAC analysis. Limnol. Oceanogr. **50:** 686–697.

TREMBLAY, L. B., T. DITTMAR, A. G. MARSHALL, W. J. COOPER, AND W. T. COOPER. 2007. Molecular characterization of dissolved organic matter in a North Brazilian mangrove porewater and mangrove-fringed estuaries by ultrahigh resolution Fourier transform-ion cyclotron resonance mass spectrometry and excitation/emission spectroscopy. Mar. Chem. **105:** 15–29, doi:10.1016/j.marchem.2006.12.015.

TZORTZIOU, M., C. L. OSBURN, AND P. J. NEALE. 2007. Photobleaching of dissolved organic material from a tidal marsh-estuarine system of the Chesapeake Bay. Photochem. Photobiol. **83:** 782–792, doi:10.1562/2006-09-28-RA-1048.

VODACEK, A., N. V. BLOUGH, M. D. DEGRANDPRE, E. T. PELTZER, AND R. K. NELSON. 1997. Seasonal variation of CDOM and DOC in the Middle Atlantic Bight: Terrestrial inputs and photooxidation. Limnol. Oceanogr. **42:** 674–686.

WARNOCK, R. E., W. W. C. GIESKES, AND S. VAN LAAR. 1999. Regional and seasonal differences in light absorption by yellow substance in the Southern Bight of the North Sea. J. Sea Res. **42:** 169–178.

WHITEHEAD, R. F., S. DE MORA, S. DEMERS, M. GOSSELIN, P. MONFORT, AND B. MOSTAJIR. 2000. Interactions of ultraviolet-B radiation, mixing and biological activity on photobleaching of natural chromophoric dissolved organic matter: A meso-cosm study. Limnol. Oceanogr. **45:** 278–291.

YALE-DAWSON, E., AND M. S. FOSTER. 1982. Seashore plants of California. California Natural History Guide Series, no. 47. University of California Press.